

Spectral line fitting of an astronomical source

S.C. Jones, D.A. Naylor, B.G. Gom and L.D. Spencer

Institute for Space Imaging Science, Department of Physics & Astronomy,
University of Lethbridge, Lethbridge AB, CA T1K 3M4 E-mail: scott.jones@uleth.ca

ABSTRACT

Astronomy is unique among the physical sciences in that virtually all information is obtained via remote sensing. Many of the techniques that have been developed for astronomy now find extensive use in terrestrial remote sensing applications. Among these, spectral line fitting provides a powerful means of extracting additional information from imaging spectroscopy. This paper presents predictions of the spectra that will be obtained from a new imaging Fourier transform spectrometer, currently under development for use at the James Clerk Maxwell Telescope. The simulation is based on spectral data obtained with a high resolution heterodyne spectrometer operating at the same telescope and over the same wavelength range, and thus provides a unique level of realism. The paper shows how, with a detailed knowledge of the instrumental line shape, it is possible to extract key spectral line information from the lower resolution Fourier transform spectrometer data.

Keywords: Heterodyne, Instrumental Line Shape, Fourier Transform Spectroscopy, Line Fitting

1 INTRODUCTION

Approximately half of the electromagnetic energy emitted by the universe occurs at submillimetre wavelengths. Unfortunately, observations at these wavelengths are extremely challenging, for two reasons: firstly, the atmosphere is opaque over most of this range, and secondly, the technology required is complex, comparable to that found in a well-equipped low temperature physics laboratory. Emission at these wavelengths takes the form of both continuum (ice, dust) and line (atomic, molecular) components. The continuum emission provides information on the nature of the emitting solid particulates and their physical properties; line emission provides information on the column abundance of the atomic and molecular species and their physical conditions. The submillimetre represents one of the last uncharted regions of the electromagnetic spectrum. To explore this domain, existing facilities are being upgraded (JCMT [7]), new facilities are coming online (Herschel [9]) and others are under development (ALMA [12]). Together, these facilities will open a new window on the submillimetre universe and allow astronomers to probe fundamental questions, such as the formation and evolution of stars and galaxies.

2 TECHNOLOGY

As the energy associated with a submillimetre photon is extremely small (~ 1 meV (1.602×10^{-22} J)), its measurement requires an exquisitely sensitive detector. In order to keep the detector noise component below the photon noise, the detector must be cooled to temperatures well below 1 K. With these constraints, the technology required differs little from that in a low temperature physics laboratory. Space-based instruments, such as the Herschel space observatory, have the advantage of not having to contend with the atmosphere, but the disadvantage of having a telescope of smaller aperture (~ 3.5 m). By contrast, the largest submillimetre ground-based telescope, the JCMT, views astronomical sources through the Earth's atmosphere, but has the advantage of having a large aperture (15 m).

Our group is currently developing an imaging Fourier transform spectrometer (FTS-2) for use with the next-generation submillimetre continuum bolometer array detector (SCUBA-2) at the JCMT [2]. In an effort to simulate the spectrum that will be observed with FTS-2, much higher resolution spectra, obtained with the recently commissioned HARP imaging spectrometer [11] have been used. While heterodyne receivers typically have resolving powers over two orders of magnitude greater than a Fourier transform spectrometer (FTS), they operate over narrow bandwidths and generally have difficulty establishing a continuum level, making them insensitive to dust emission. By contrast, an FTS is well suited for the simultaneous measurement of continuum and line emission, albeit at a lower spectral resolution.

3 THE JCMT

The JCMT, commissioned in 1987, is the world's largest submillimetre telescope. It is located on the summit of Mauna Kea in Hawaii at an altitude of 4092 m. In recent years, the instrument suite at the JCMT has been upgraded

to accommodate the recent advances in heterodyne and bolometric array detector development. This has resulted in two new facility instruments: HARP [11] and SCUBA-2 [2].

3.1 HARP

HARP [11] is a 16-element heterodyne array receiver, arranged in a 4x4 pixel configuration, that was designed and built at the University of Cambridge to operate in the 325-375 GHz (10.8-12.5 cm⁻¹) range with an instantaneous spectral resolution of ~1 MHz (~34 μcm⁻¹). HARP uses an autocorrelation spectrometer and imaging system called ACSIS (Auto-Correlation Spectrometer and Imaging System) which, together with the large aperture telescope, provides large sensitive spectral line maps of astronomical sources. However, because the baselines are removed before stitching together the individual spectral scans in the heterodyne instrument, HARP is unable to extract the continuum emission.

3.2 SCUBA-2

The other new JCMT facility instrument is SCUBA-2, the next generation of bolometric camera. Bolometers are essentially very sensitive thermometers, which measure changes in temperature by virtue of a change in resistance. Typically, they consist of an absorbing substrate and a detecting element. In bolometric design, the challenge is to find a material with the highest temperature coefficient of resistance, α . Historically, neutron transmutation doped (NTD) germanium has been the thermometer of choice, because of its high α , but in recent years it has been recognized that the transition edge of a superconductor has an α about a hundred times greater, and now the challenge is to design a detector array that will operate on the midpoint of this transition. Unlike its predecessor SCUBA [3], which employed 128 NTD detectors, SCUBA-2 features approximately 10,000 pixels in its transition-edge sensor (TES) array. Once commissioned, it is expected that SCUBA-2 will provide a 1000-fold increase in mapping speed over its predecessor.

3.3 FTS-2

Building on experience gained with single pixel FTS at the JCMT, our group is building a Fourier transform spectrometer (FTS-2) for use with the SCUBA-2 bolometric camera to add an imaging spectroscopic capability. Detailed information on the optical design of FTS-2 is presented elsewhere [8]. FTS-2 is a large instrument (2.4m x 0.8m x 1.4m) with a mass of ~500 kg that sits between the elevation bearing of the telescope and the SCUBA-2 transfer optics. When commissioned, it will provide simultaneous imaging spectroscopic observations in the 850 and 450 micron bands with user selectable spectral resolving powers between 10 and 5000 [8].

4 SPECTRAL SIMULATION

In order to simulate the spectral data that will be generated by FTS-2, the JCMT Spectral Legacy Survey [10] team have kindly made available a complete spectral scan of the galactic source G34.3, a well-studied, ultracompact HII region with an associated hot molecular cloud core [5]. It is comprised of three sub-regions, of which two are ultracompact and one is compact. It has a cometary morphology, and is located at an estimated distance from Earth of 3.7 kpc. The top trace in Figure 1 shows the high resolution heterodyne spectrum of G34.3. Many molecular emission lines can be readily identified, including the CO 3-2 transition at 11.53 cm⁻¹. The goal of this work was to predict the appearance of this spectrum as measured with FTS-2.

4.1 FTS Simulated Spectrum

A Fourier transform spectrometer has the best Instrumental Line Shape (ILS) of any spectrometer [1], given by the cardinal sine (sinc):

$$F(\sigma) = \frac{\sin(2\pi\sigma L)}{2\pi\sigma L} \quad (1)$$

where σ is the wavenumber, and L is the maximum optical path difference (OPD) between beams in the interferometer. The full width at half maximum (FWHM) of the FTS ILS is

$$\Delta\sigma_{FTS-FWHM} \cong \frac{1.207}{2L} \quad [cm^{-1}]. \quad (2)$$

As expected, the spectral resolution is inversely proportional to the maximum OPD of a particular interferogram. For the purposes of this paper we have chosen a spectral resolution of 0.01 cm⁻¹ for our sinc function, to match the expected performance of FTS-2. Convolution of this kernel with the heterodyne data (upper trace in Figure 1) results in

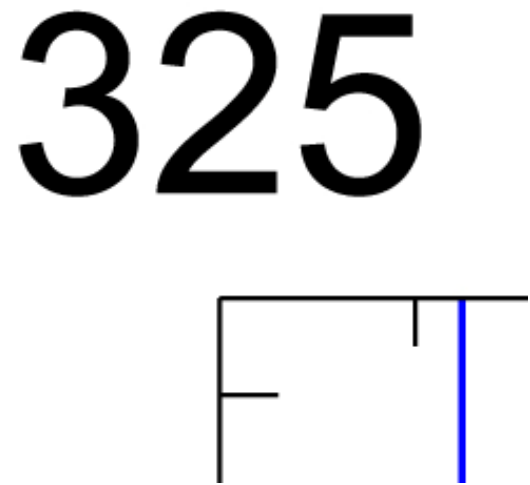


Figure 1. HARP G34.3 spectrum (top), with each of the eleven lines for which spectral fitting was attempted identified by the blue vertical lines. The middle curve is the spectrum upon convolution with the ILS of the FTS, to a super-sampled spectral resolution of 1 MHz ($34 \mu\text{m}^{-1}$). At bottom (filled circles) the spectrum is further sub-sampled to a spacing of 0.01 cm^{-1} , the expected resolution for FTS-2.

the data but this is a direct result of the extended sidelobes of the convolution kernel (shown in Figure 2), which sum constructively or destructively at different frequencies depending upon the spectral line content of the input spectrum. The final simulation product is obtained by down-sampling the centre trace to a spectral resolution of 0.01 cm^{-1} , which is shown in the lower trace in Figure 1. Although this resulting spectrum appears to the untrained eye to be noisier than the centre trace, it has exactly the same Fourier components and thus the same information content. The bottom trace of Figure 1 thus represents the best, most realistic simulation of an FTS spectrum from G34.3.

5 SPECTRAL LINE FITTING

One of the challenges with FTS data is to use its well-known ILS to recover spectral information by a multi-component fitting routine. The software used was developed in the Interactive Data Language (IDL) [4], and uses the Levenberg-Marquardt least squares method to perform the fit. The convergence criterion is set by an appropriate threshold in the change in the reduced chi-squared value at each iteration in the algorithm. In the following analysis it has been assumed that the instrumental line shape is well-defined and stable, as has been shown to be the case from a lengthy heritage of FTS observations conducted at the JCMT. The ILS itself can be determined either from absorption features provided by a gas cell or from an unresolved spectral line source such as a laser or a photomixer [6]. Thus, to fit the spectrum only the line centre and intensity are required. Moreover, since the heterodyne data are baseline corrected, there is no requirement to fit an underlying Planck continuum, although this could be readily

included. The eleven strongest lines in the G34.3 heterodyne spectrum (upper trace of Figure 1) were input to the fitting procedure. In the fitting routine, the line centre and amplitude were allowed to vary while the ILS is fixed. Upon convergence the fitting routine returned the line centre and intensity. Figure 2 presents a pictorial summary of the eleven components fit to the input spectrum. In Figure 3, the eleven sinc components are summed into a single trace (centre) which is compared with the sub-sampled input spectrum (top). The resulting residual is also shown (bottom).

The results of the fitting procedure are summarized in Table 1, which compares the line centres and integrated line areas as derived from the heterodyne data and the results from the fitting routine applied to the simulated FTS data. The heterodyne data were regarded as the reference. The line centres were measured from the raw data to an accuracy of ~ 1 MHz ($3.36\text{E-}5 \text{ cm}^{-1}$); the integrated flux (mK cm^{-1}) was determined over a narrow frequency range around the emission line, typically less than 10 MHz. The corresponding line centres (σ_0) and integrated line flux ($A/2L$) for the FTS data were derived directly from the individual fitted sinc functions:

$$\int_{-\infty}^{\infty} A \frac{\sin(2\pi(\sigma - \sigma_0)L)}{2\pi(\sigma - \sigma_0)L} dx = \frac{A}{2L}, \quad (3)$$

where A is the amplitude of the spectral line. Table 1 shows that there is excellent agreement between the retrieved values for the line centre and integrated flux, as determined from the fitting method, and the corresponding values

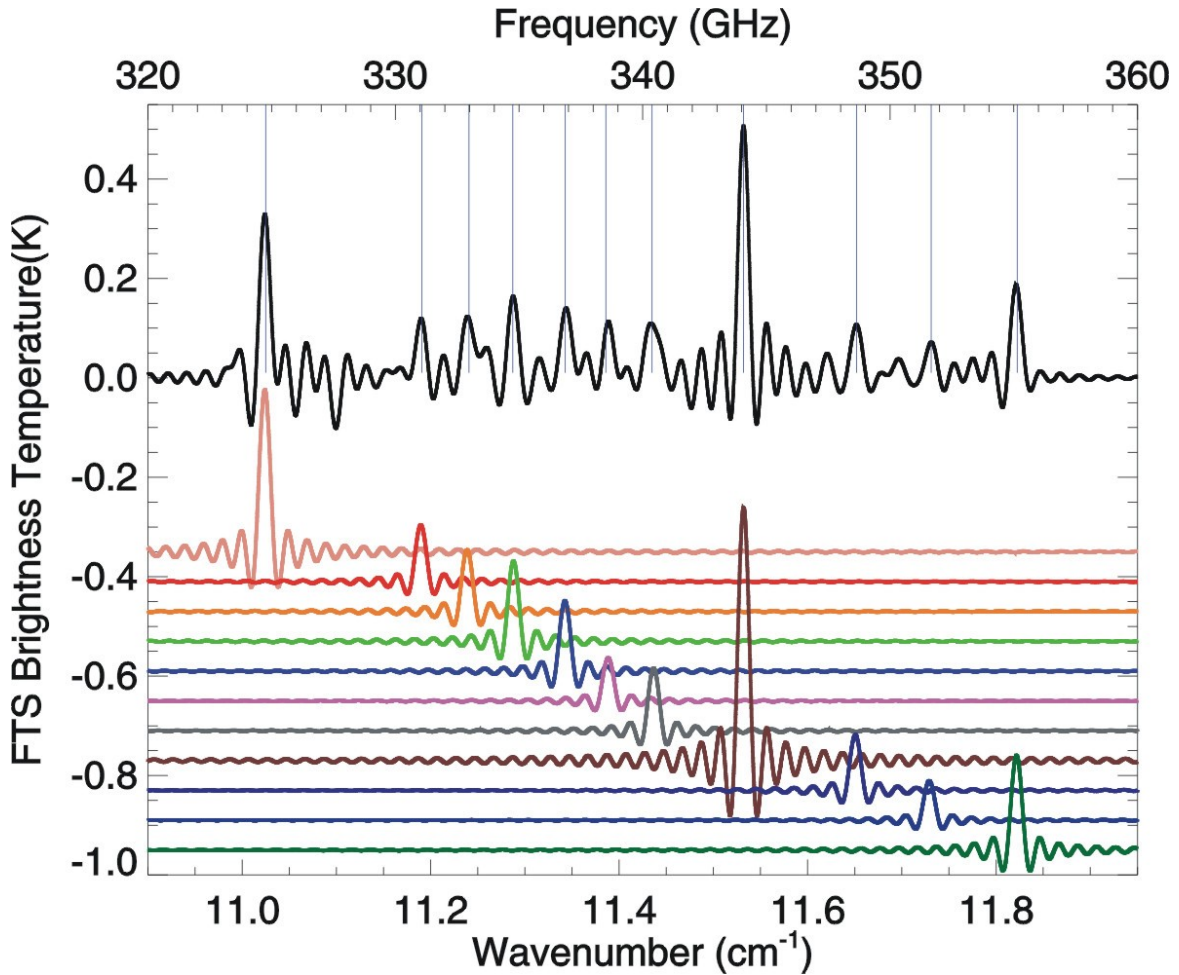


Figure 2. The convolved spectrum of the same spectral resolution as Figure 1 (1 MHz ($34 \mu\text{m}^{-1}$)), with the vertical blue lines showing, as before, the positions of the fitted spectral lines. The bottom part of the figure illustrates the sinc functions

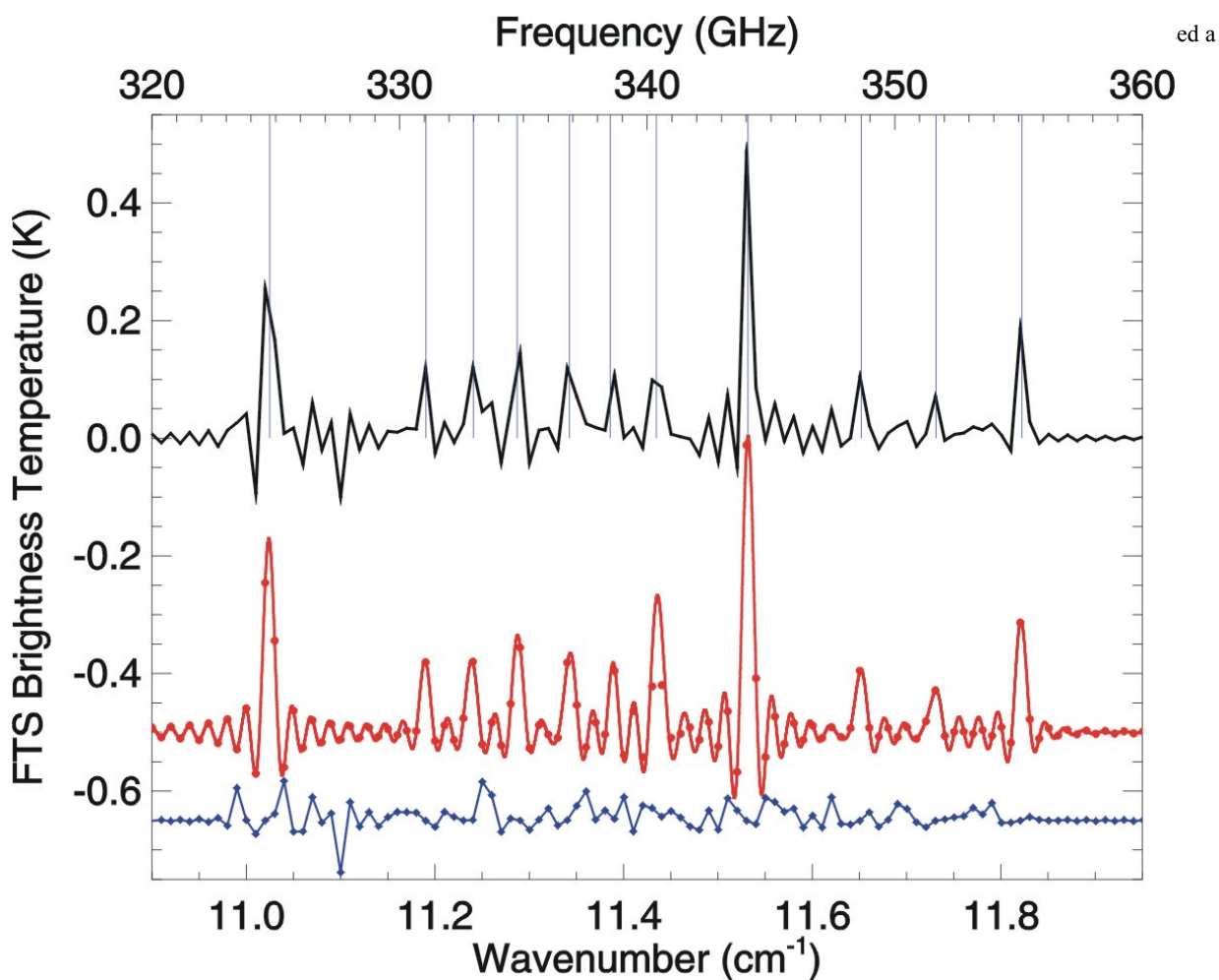


Figure 3. The recovered 11-line FTS-2 simulated G34.3 spectrum. The top curve shows the spectrum at the FTS-2 resolution of 0.01 cm^{-1} . The middle curve (filled circles) presents the same spectrum at the higher, 1 MHz ($34 \text{ } \mu\text{cm}^{-1}$) resolution, while the lower curve (filled diamonds) shows the residual spectral error. All curves are arbitrarily offset for clarity.

Line	Het. Centre (cm^{-1})	FTS centre (cm^{-1})	Difference (cm^{-1})	Difference (fraction of resolution element)	Het. Area (mK cm^{-1})	FTS Area (mK cm^{-1})	Difference (mK cm^{-1})	Percentage Error
1	11.02489	11.0239	0.00099	0.099	3.0953086	3.1992356	0.103927	3.3575651
2	11.19061	11.18947	0.00114	0.114	1.1486849	1.2611542	0.112469	9.7911359
3	11.24069	11.23861	0.00208	0.208	1.0736124	1.2233868	0.149774	13.95051
4	11.28716	11.28781	0.00065	0.065	1.6018771	1.4627277	0.139149	8.6866464
5	11.34269	11.34243	0.00026	0.026	1.7279041	1.5189525	0.208952	12.092778
6	11.38587	11.38831	0.00244	0.244	0.6831963	0.7002658	0.01707	2.4984766

Table 1. A comparison of recovered FTS line centres and integrated areas for heterodyne and FTS-simulated spectra, with the associated differences/errors shown in the adjacent columns. The line amplitudes were measured in brightness temperature, the value for which a blackbody's intensity matches that of a grey body at a certain frequency or wavenumber.

from the heterodyne spectrum. In all cases, the analysis is able to determine line centres to an accuracy greater than the resolution of the FTS. As expected, the error in the retrieved integrated line fluxes is lowest for the strongest lines.

To explore the impact of noise on the simulated FTS spectrum, normally-distributed white noise, with a mean of zero (generated using the Box-Muller method), was added to the sum of sinc fits shown in the middle of Figure 3, and the fitting process was repeated. The noise amplitude was taken to be ten percent of the largest peak in the upper trace of Figure 3, namely the CO 3-2 line at 11.53 cm^{-1} . Additionally, so as to avoid any rogue data values, individual noise spectra were generated one hundred times such that each iteration resulted in a different random noise being added to the simulated spectrum. As before, the fitting routine returned line center and integrated flux information for each of the eleven lines. The results of this analysis are summarized in Figures 4 and 5, which display the error in the line centre and the integrated line flux as a function of the integrated line intensity, derived from the input heterodyne data. The error has been calculated as the absolute value of the difference between the retrieved fitted parameters for the FTS-simulated data and the FTS-simulated data to which noise has been added. As expected, the errors are inversely proportional to the intensity of the individual lines. Overplotted on these figures is a reciprocal function which shows the theoretical prediction of the variation of errors as a function of integrated line strength from a spectral signal-to-noise argument.

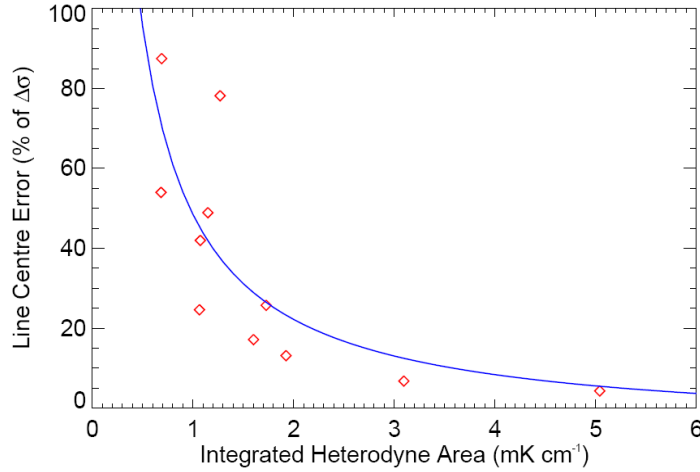


Figure 4. The uncertainty in the line centre clearly follows an inverse relationship with the integrated spectral line area.

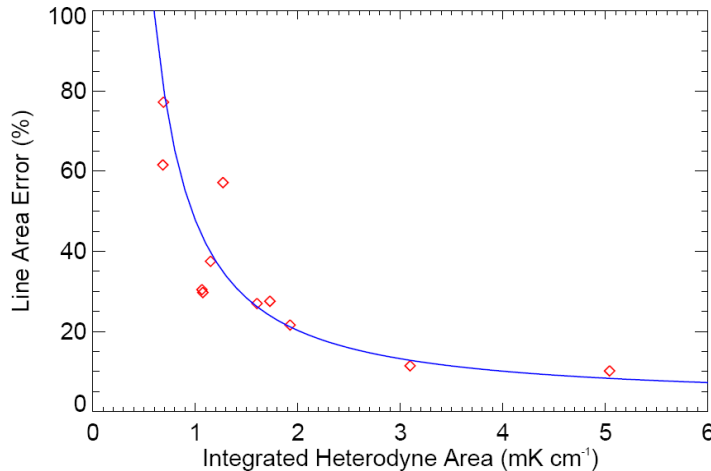


Figure 5. The uncertainties in the line area also follow an inverse relationship with the integrated spectral line area.

6 CONCLUSIONS

The spectra that we have obtained through convolution of the high-resolution HARP data with a low-resolution sinc function represent the most realistic prediction of the spectra that will be obtained with SCUBA-2 (FTS-2). This paper has shown that with a knowledge of the ILS, it is possible to recover key spectral parameters of line centre and integrated line flux. While line fitting is a standard tool of spectroscopists, the methods used in this paper are robust in that they perform well upon the addition of white noise into the spectrum. Furthermore, the procedure that has been established here will not only find extensive use with the SCUBA-2 (FTS-2) data, but also with spectroscopic data from the SPIRE FTS on board the Herschel observatory [8], whose bandpass is more than an order of magnitude greater and will therefore measure emission lines from numerous ionic, atomic and molecular species as well as continuum emission simultaneously.

ACKNOWLEDGMENTS

The authors would like to acknowledge the entire Spectral Legacy Survey (SLS) [9] team, in particular Rene Plume, at the University of Calgary, who suggested the G34.3 source, and Helen Roberts, from Queen's University, Belfast, who kindly processed the raw data through the HARP pipeline before handing it over to us. D.A.N. also thanks NSERC and CFI.

REFERENCES

1. Davis, S.P., M.C. Abrams and J.W. Brault, 2001. Fourier Transform Spectrometry. Academic Press. (0120425106). 262p.
2. Holland, W.S., W.D. Duncan, B.D. Kelly, K.D. Irwin, A.J. Walton, P.A.R. Ade and E.I. Robson, 2003. SCUBA-2: A large format submillimetre camera on the James Clerk Maxwell Telescope. *Proc. SPIE*. 4855: 1-18
3. Holland, W.S. et al., 1999. SCUBA: a common-user submillimetre camera operating on the James Clerk Maxwell Telescope. *Mon. Not. R. Astron. Soc.* 303: 659-672.
4. Interactive Data Language, Research Systems Inc., 2004.
5. Macdonald, G.H., A.G. Gibb, R.J. Habing and T.J. Millar, 1996. A 330-360 GHz spectral survey of G34.3+0.15. I. Data and physical analysis. *Astronomy & Astrophysics Supplement Series*. 119: 333-367
6. Matsuura, S. et al., 2000. A Photonic Local Oscillator Source for Far-IR and Sub-mm Heterodyne Receivers. The Institute of Space and Astronomical Science Report SP No 14
7. Murdin, P., 2001. Encyclopedia of Astronomy and Astrophysics: James Clerk Maxwell Telescope. Institute of Physics Publishing, Bristol. (1561592684). 2500p.
8. Naylor, D.A., B.G. Gom and B. Zhang, 2006. Preliminary design of FTS-2: an imaging Fourier transform spectrometer for SCUBA-2. *Proc. SPIE: Astronomical Telescopes and Instrumentation*. 6275
9. Pilbratt, G.L., 2008. Herschel Mission Overview and Key Programmes. *Proc. SPIE: Space Telescopes and Instrumentation I – Optical, Infrared, and Millimetre Wave*. 7010:701002-1-12, 2008
10. Plume, R. et al., 2007. The JCMT Spectral Legacy Survey. *Publications of the Astronomical Society of the Pacific*. 119 (851): 102-111
11. Smith, H., et al., 2008. HARP: a submillimetre heterodyne array receiver operating on the James Clerk Maxwell Telescope. *Proc. SPIE: Millimetre and Submillimetre Detectors and Instrumentation for Astronomy IV*. 7020:70200Z
12. Tarengi, M., 2008. The Atacama Large Millimetre/Submillimetre Array: overview & status. *Astrophys. Space Sci.* 313: 1-7

